starling. *Ardea* **77,** 75–86 (1989).
7. Gentner, T. Q. & Hulse, S. H. Perceptual mechanisms for individual vocal recognition in European starlings, *Sturnus vulgaris. Anim. Behav.* **56,** 579–594 (1998).
8. Vates, G. E., Broome, B. M., Mello, C. V. & Nottebohm, F. Auditory pathways of caudal telencephalon and their relation to the song system of adult male zebra finches. *J. Comp. Neurol.* **366,** 613–642 (1996).
9. Müller, C. M. & Leppelsack, H. J. Feature-extraction and tonotopic organization in the avian auditory forebrain. *Exp. Brain Res.* **59,** 587–599 (1985).
10. Sen, K., Theunissen, F. E. & Doupe, A. J. Feature analysis of natural sounds in the songbird auditory forebrain. *J. Neurophysiol.* **86,** 1445–1458 (2001).
11. Margoliash, D. Acoustic parameters underlying the responses of song-specific neurons in the white-crowned sparrow. *J. Neurosci.* **3,** 1039–1057 (1983).
12. Margoliash, D. Preference for autogenous song by auditory neurons in a song system nucleus of the white-crowned sparrow. *J. Neurosci.* **6,** 1643–1661 (1986).
13. Leppelsack, H. J. & Vogt, M. Responses of auditory neurons in forebrain of a songbird to stimulation with species-specific sounds. *J. Comp. Physiol.* **107,** 263–274 (1976).
14. Scheich, H., Langner, G. & Bonke, D. Responsiveness of units in the auditory neostriatum of the guinea fowl (numida-meleagris) to species-specific calls and synthetic stimuli, 2: discrimination of iambus-like calls. *J. Comp. Physiol.* **132,** 257–276 (1979).
15. Wang, X. & Kadia, S. C. Differential representation of species-specific primate vocalizations in the auditory cortices of marmoset and cat. *J. Neurophysiol.* **86,** 2616–2620 (2001).
16. Rauschecker, J. P., Tian, B. & Hauser, M. Processing of complex sounds in the macaque nonprimary auditory cortex. *Science* **268,** 111–114 (1995).
17. Gilbert, C. D., Sigman, M. & Crist, R. E. The neural basis of perceptual learning. *Neuron* **31,** 681–697 (2001).
18. Bakin, J. S. & Weinberger, N. M. Classical conditioning induces CS-specific receptive field plasticity in the auditory cortex of the guinea pig. *Brain Res.* **536,** 271–286 (1990).
19. Recanzone, G. H., Schreiner, C. E. & Merzenich, M. M. Plasticity in the frequency representation of primary auditory cortex following discrimination training in adult owl monkeys. *J. Neurosci.* **13,** 87–103 (1993).
20. Kilgard, M. P. & Merzenich, M. M. Order-sensitive plasticity in adult primary auditory cortex. *Proc. Natl Acad. Sci. USA* **99,** 3205–3209 (2002).
21. Kay, L. M. & Laurent, G. Odor- and context-dependent modulation of mitral cell activity in behaving rats. *Nature Neurosci.* **2,** 1003–1009 (1999).
22. Kilgard, M. P. & Merzenich, M. M. Plasticity of temporal information processing in the primary auditory cortex. *Nature Neurosci.* **1,** 727–731 (1998).
23. Logothetis, N. K., Pauls, J. & Poggio, T. Shape representation in the inferior temporal cortex of monkeys. *Curr. Biol.* **5,** 552–563 (1995).
24. Kobatake, E., Wang, G. & Tanaka, K. Effects of shape-discrimination training on the selectivity of inferotemporal cells in adult monkeys. *J. Neurophysiol.* **80,** 324–330 (1998).
25. Rainer, G., Asaad, W. F. & Miller, E. K. Selective representation of relevant information by neurons in the primate prefrontal cortex. *Nature* **393,** 577–579 (1998).
26. Rainer, G. & Miller, E. K. Effects of visual experience on the representation of objects in the prefrontal cortex. *Neuron* **27,** 179–189 (2000).
27. Tchernichovski, O., Mitra, P. P., Lints, T. & Nottebohm, F. Dynamics of the vocal imitation process: how a zebra finch learns its song. *Science* **291,** 2564–2569 (2001).

Supplementary Information accompanies the paper on **www.nature.com/nature**.

Acknowledgements We thank F. E. Theunissen for generously providing software and assistance for calculating STRFs, M. Konishi and L. M. Kay for valuable critiques of the manuscript, Z. Chi and S. Shea for helpful discussions, and D. Baleckaitis for histology. This work was supported by grants from the National Institutes of Health to T.Q.G. and D.M.

Competing interests statement The authors declare that they have no competing financial interests.

Correspondence and requests for materials should be addressed to T.Q.G. (t-gentner@uchicago.edu).

Neural correlates of implied motion

Bart Krekelberg[1], Sabine Dannenberg[2], Klaus-Peter Hoffmann[2], Frank Bremmer[2,3] & John Ross[4]

[1]*Vision Center Laboratory, The Salk Institute, La Jolla, California 92037, USA*
[2]*Department of Neurobiology, Ruhr University, D-44780 Bochum, Germany*
[3]*Cognitive Neuroscience Laboratory, Department of Neurophysics, Philipps University Marburg, D-35032 Marburg, Germany*
[4]*School of Psychology, The University of Western Australia, Nedlands, WA 6907, Australia*

Current views of the visual system assume that the primate brain analyses form and motion along largely independent pathways[1]; they provide no insight into why form is sometimes interpreted as motion. In a series of psychophysical and electrophysiological experiments in humans and macaques, here we show that some form information is processed in the prototypical motion areas of the superior temporal sulcus (STS). First, we show that STS cells respond to dynamic Glass patterns[2], which contain no coherent motion but suggest a path of motion[3]. Second, we show that when motion signals conflict with form signals suggesting a different path of motion, both humans and monkeys perceive motion in a compromised direction. This compromise also has a correlate in the responses of STS cells, which alter their direction preferences in the presence of conflicting implied motion information. We conclude that cells in the prototypical motion areas in the dorsal visual cortex process form that implies motion. Estimating motion by combining motion cues with form cues may be a strategy to deal with the complexities of motion perception in our natural environment.

Many studies have shown that the ventral part of the primate brain specializes in the processing of complex visual form, whereas the dorsal part of the brain specializes in the analysis of visual motion[1]. Some, however, have questioned this strict division of labour. Geisler[4], for instance, showed that humans use traces of motion, which he termed motion streaks, to improve their detection of moving objects. Cells in the primary visual cortex could underlie this ability[5,6]. Kourtzi and Kanwisher[7] showed that static images that imply motion (such as a basketball player about to throw a ball) activate areas in the human brain that process motion information (hMT+). Finally, Ross *et al.*[3] demonstrated that humans can perceive form itself as motion: subjects perceived coherent motion in sequences of rotational Glass patterns[2] that contain no coherent motion.

Glass patterns consist of a collection of randomly placed pairs of dots, all oriented along a common path (Fig. 1a). This path corresponds to the perceived path of motion. We refer to this type of motion, which is ambiguous in direction, as implied motion; it is implied by the form of the global pattern, not carried by directed motion signals (see Supplementary Information A). The perception of coherent motion in Glass patterns depends critically on the separation (called the Glass shift) between the elements of the dot pairs. For small and large shifts, the sequence of patterns is perceived as random noise; only for an intermediate range does the percept of motion arise (see Fig. 2 in Ross *et al.*[3]). By aligning dot pairs along different paths, various types of global illusory motion can be created: translations, rotations, and expansions and contractions. The global organization in Glass patterns is particularly strong for rotations[3,8] and expansions[9]. Cells in visual area V1 in macaques have recently been shown to respond selectively to the weak locally oriented features[10], allowing them to pass on this information to extrastriate areas for the analysis of global form. These properties make Glass patterns particularly suitable for our experiments. Nevertheless, we believe that they are merely instances of a general class of stimuli that provide motion information by means of their form[9].

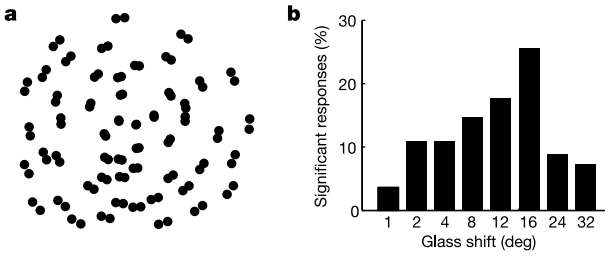

Figure 1 Optimal Glass patterns activate the STS population. **a**, A rotational Glass pattern. Presenting many randomly chosen patterns like this, one after another, leads to the impression of rotational motion[3]. **b**, The histogram shows how likely it was that the presentation of a Glass pattern with a given shift evoked a response in any of the STS cells that was significantly larger than the random-noise control condition.

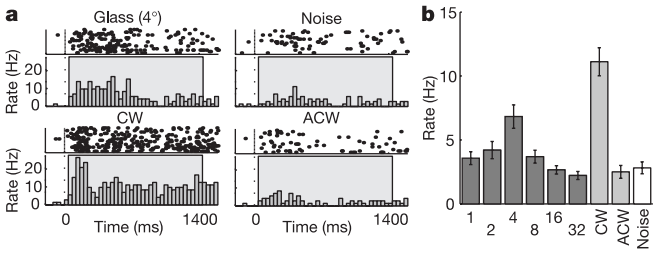

Figure 2 Responses to implied motion in a single cell. **a**, Raster and peri-stimulus-time histogram for responses to a Glass pattern with a 4° shift, a noise pattern, and clockwise (CW) and anticlockwise (ACW) rotation. **b**, Average firing rates in the stimulation period indicated by the grey area in **a**. The numbers on the ordinate refer to the Glass shift in degrees.

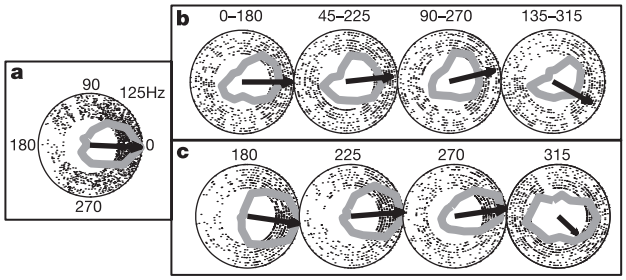

Figure 4 Interactions between real and implied motion in a single cell. **a**, Polar direction tuning plot for a random dot pattern on a circular pathway. Dots represent single spikes recorded while the pattern moved in that direction, corrected for the latency of the cell. The solid grey curve represents the mean firing rate (the full radius represents 125 Hz in all polar plots), the arrow the preferred direction. **b**, Direction tuning for a combination of circular pathway motion with a Glass pattern oriented along the axis indicated above the plots. **c**, Direction tuning for circular pathway motion combined with translational motion in the direction indicated above the plots.

We have found a neural correlate of the global implied motion percept in the dorsal stream of the macaque visual cortex. While the monkeys fixated the centre of a screen, we recorded from cells in the medial (MT) and medial superior (MST) temporal areas of the superior temporal sulcus. We presented sequences of rotational Glass patterns (see Methods) with a varying amount of Glass shift. Humans perceived the patterns with the smallest and largest shift as random noise; only the patterns in the centre of the tested range reliably led to a coherent rotational motion percept, albeit with an ambiguous direction. Figure 2 shows a cell that fired maximally when the Glass shift was such that humans perceived coherent rotation. For small or very large Glass shifts, however, the firing of the cell was indistinguishable from its response to random noise. Of the 109 cells tested in this paradigm, 18 (17%) showed such a tuning for Glass shift. Figure 2 also shows that this cell's response to Glass patterns was more variable over time. This was typical. Because the direction of motion in these patterns is ambiguously clockwise and anticlockwise, one may in fact have predicted that the neurons should show clockwise responses on some trials and anticlockwise responses on other trials. We could show that this was indeed often the case (see Supplementary Information B).

Next, we determined whether the STS population as a whole was sensitive to those Glass patterns that we perceived as coherent motion. Figure 1b shows the probability that a particular Glass shift evoked a mean response larger than the response to random noise (analysis of variance on ranks, followed by a post-hoc test, 109 cells). This confirms that Glass patterns outside the central range tended to evoke a response that was indistinguishable from the response to random noise. In the centre of the Glass shift range, where we perceived coherent motion, more responses were significantly larger than the response to random noise.

To further demonstrate the equivalence of implied and real motion, we determined whether a cell's preference for expanding or rotating flow patterns predicted its preference for expansion or rotational Glass patterns. The trend ($P = 0.055$) that 20 out of 32 cells thus tested preferred the same type of motion in the real motion domain as in the implied motion domain suggests that implied motion activated the appropriate cells in the STS.

If indeed the same neurons process implied and real motion cues, one would expect these cues to interact perceptually. In other words, it should be possible to change the perceived direction of real motion by giving conflicting implied motion information. We first tested this in a psychophysical experiment in humans.

Subjects judged the direction of global motion in displays containing both real-motion and translational Glass patterns. Figure 3a shows by how much the judged direction of global motion was deflected away from the true direction and attracted towards the direction implied by the Glass patterns. We call the difference in angle between the implied motion and the true direction of motion the conflict angle. When the conflict angle was small—less than 20°—the deflection was almost half the angular difference. This indicates that, under these circumstances, the implied motion and the real motion had almost equal influence on the judged direction of motion. As the conflict angle widened, the influence of pair orientation on judged motion direction weakened. Near 90° the Glass pattern had only a small influence—repulsive, not attractive—on the judged direction of motion. An even stronger influence of form on motion was found for spiral Glass patterns (Supplementary Information C).

Next, we investigated the interaction between real and implied motion in STS cells. First, we determined directional tuning curves for each cell by showing a field of random dots on a circular motion

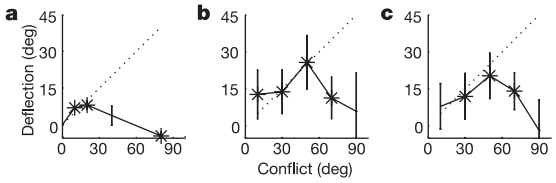

Figure 3 Interactions between real and implied motion. **a**, Human perception. The deflection of direction—averaged over three observers—is shown as a function of the conflict angle. **b**, The average STS population deflection as a function of the conflict between the orientation of the Glass pattern and the PD of the cell. **c**, The deflection as a function of the conflict between the axis of real motion and the PD. In all three panels, a positive deflection indicates a change towards the implied motion, asterisks indicate statistical significance, the dotted line represents the predicted deflection if real and implied motion had equal influence, and error bars represent 95% confidence intervals.

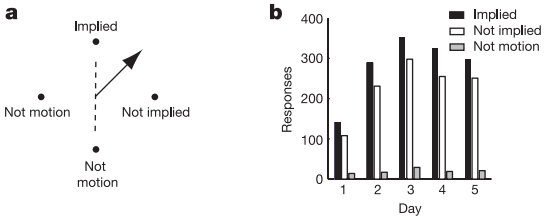

Figure 5 Monkey psychophysics. **a**, The arrow indicates the direction of real motion, the dashed line the orientation of the Glass pattern. The dots are saccade targets that the monkey used to indicate his perceived direction of motion. In this example (45° real motion with a vertical Glass pattern), the monkey's decisions can be interpreted as indicated by the labels. **b**, Results, averaged over all directions of motion, on five consecutive days.

trajectory in the fronto-parallel plane. This gave us a preferred direction (PD) of motion for the neuron[11,12]. Second, we mapped the directional tuning again, but now while a translational Glass pattern oriented along one of the cardinal axes was shown transparently. Of the 62 visually responsive cells recorded in this paradigm, the Glass patterns significantly affected the preferred direction of 16 (26%) cells (one-way analysis of variance on ranks, $P < 0.05$). Third, we mapped the directional tuning again, but now while a real translating flow field was presented transparently. The axis of motion of the real translating flow field significantly affected the preferred direction of 37 neurons (60%). Assuming that cells represent the direction of motion for which they respond best, our psychophysical findings predicted that Glass patterns that were orthogonal to a cell's PD (large conflict angle) should have only a small influence on the PD. For Glass patterns that were nearly but not quite parallel to the PD of a cell (small conflict angle), we expected the PD to shift towards the implied motion cue in the Glass pattern. Figure 4 shows an example of a cell that fitted this prediction. The cell preferred rightwards motion (Fig. 4a). As expected, the combination of multiple motion signals (Fig. 4b, c) resulted in a reduced firing rate[13,14] and broader tuning curves. Nevertheless, when direction tuning was assessed in the presence of a 135–315° Glass pattern or a 315° real motion pattern, this cell's preferred direction shifted consistently towards 315°. For this cell, the effect of all other directions was smaller. Moreover, the effects of real and implied motion were similar. For individual cells, the changes in PD were often small and variable; in Fig. 4, only the change in PD with a 135–315° Glass pattern is significantly different from zero. At the population level, however, the effects were clearer. Figure 3b, c shows population averages of the deflection as a function of the conflict angle. Figure 3b demonstrates that Glass patterns that were close to the preferred direction of the cell changed the preferred direction for the transparent stimulus. For small conflicts between the implied motion and real motion signals, the influence of implied motion was as strong as that of real motion; the represented direction of motion was the vector average. For larger conflicts, however, the cells demonstrated winner-take-all behaviour: they ignored the implied motion. Figure 3c shows the same calculations for the interaction of two transparently shown directions of real motion. Here, too, small conflicts lead to deflections of the preferred direction, whereas large conflicts show winner-take-all behaviour. In the human psychophysics we found that large conflicts lead to a small repulsive effect; even though there is a small negative deflection in the motion–motion interactions in the STS (Fig. 3c), this effect was not statistically significant. These data not only show a neural correlate of the psychophysical experiment in Fig. 3a, they also show that the influence of implied motion on real motion (Fig. 3b) is very similar to the influence of real motion on real motion (Fig. 3c). This gives further support to our claim that the visual system's processing of implied motion is very similar to that of real motion.

The interaction between real and implied motion allowed us to come full circle and test whether monkeys perceived implied motion. We trained monkey T on a four-alternative forced-choice direction-discrimination task (Fig. 5a). During the training phase, random dots moved in one of eight directions for 1 second. Then, four dots appeared and the monkey reported his perceived direction of motion by making a saccade to one of the dots. Performance reached ~80% correct. We then tested how a simultaneously presented translational Glass pattern influenced the decisions. For example, we presented 45° motion transparently with a vertical Glass pattern and showed saccade targets only for the cardinal directions. Our human psychophysical data predicted that the vertical Glass pattern should cause an upward motion bias in the 45° motion stimulus. Hence, a decision for the upward motion direction would support the implied motion hypothesis (an 'implied motion' decision), a decision for the rightward motion direction, however, counted against the hypothesis ('not-implied'). A decision for either left or downward motion is evidence that the monkey was not paying attention to the motion at all ('not-motion'). In ambiguous motion trials, the reward was random at a rate proportional to the monkey's performance on interleaved trials in which only unambiguous real motion was shown. We performed this experiment on five consecutive days and consistently found a significant ($P < 0.05$) implied motion bias for all motion directions. On average, the monkey was ~11% more likely to make a decision in the implied motion direction than orthogonal to it (Fig. 5b). The 'not-motion' decisions were rare. Hence, even on the randomly rewarded trials, the monkey attempted to perform a motion direction task. The bias towards the implied motion direction confirms that form biases motion percepts in the macaque as it does in humans.

The responses we find may be related to the orientation-selective responses in MT that have been described before[15–17]. Given that MT inactivation impairs direction but not orientation discrimination[18,19], however, the relevance in MT of orientation tuning *per se* is somewhat mysterious. The preference of some cells in MT for motion parallel to their preferred orientation is commonly interpreted in terms of the intersection of constraints model[16]. But, as Geisler *et al.* have pointed out, it could also be interpreted as sensitivity to the motion implied by streaks. Motion streaks provide the best motion information at high speeds, where estimates of real motion become less reliable; hence these motion mechanisms may in fact be complementary[4,5].

The unity of perception requires that sooner or later information on form be combined with information on motion. Our results show that at least some combination occurs not after the dorsal stream has completed its processing of motion signals, but while it is doing so. Taken together with the data of Kourtzi and Kanwisher[7], it thus appears that many hints of motion, like the oriented pairs in our Glass patterns, modulate cells in the motion areas of human and monkey brains. This may reflect a strategy that combines form with motion information to survive in an environment in which combinations of object motion and self motion, occlusion, and transparency complicate the tasks our visual system has to solve. □

Methods

Human psychophysics

Stimuli were displayed on a Hitachi Accuvue 4821 monitor (120 Hz, 800 pixels × 600 pixels) with a Cambridge Research Systems VSG2/4 graphics card. Noisy translational Glass patterns, composed of white dots (diameter 5′; 93 cd m^{-2}) were displayed on a circular grey disc (diameter 14.5°; 21.5 cd m^{-2}). The first pattern in each sequence of 10 was produced by randomly positioning the first dot of each pair, then placing its partner 20′ away, either at the signal angle for signal pairs, or at a random angle for noise pairs. Subsequent patterns were made by moving the appropriate proportion of pairs and randomly replacing the remainder. Motion step size was 20′ and new patterns were shown with 12 Hz, giving a dot speed of 4° s^{-1}.

Procedure

Motion direction was 15°, 30°, 45° or 60° from horizontal, and the orientation of Glass pairs deviated from each motion direction (positively or negatively) by 0°, 10°, 20°, 40° or 80°; 25% of pairs moved in the signal direction and 50% were at the signal orientation. Subjects reported the direction of global motion verbally or by mouse-click. Results were averaged over four judgments. Two subjects were unaware of the purpose of the experiment; one was an author.

Monkey physiology

We used two male macaques (C and T). Animal treatment was in accordance with European Community (86/609/ECC) and NIH guidelines. We recorded 168 cells in the medial temporal and medial superior temporal areas in two hemispheres. Not every paradigm could be recorded for every cell. Identification of areas on the basis of MR images, chamber position, electrode depth, the large fraction of directionally selective cells with small receptive fields (MT) or a preference for flow fields and large receptive fields (MST) led to the estimate that one-third of cells were in MT and two-thirds were in MST. We found no clear differences in the responses to the Glass patterns and therefore treated them as a single population, referred to as STS. The monkey fixated a small (<0.5°) central red dot. Fixation within 2° was monitored with an eye-coil system (500 Hz, accuracy ~1′). A frame in a Glass sequence consisted of 50 randomly positioned pairs of dots (diameter ~0.25°) in the central 30° (monkey C) or 15° (monkey T). In rotational Glass patterns, these were oriented along concentric circles around the fixation spot. In translations, the pairs were oriented horizontally (0°) or at 45°, 90° or 135°. In expansions, the pairs were

oriented along radii centred at fixation. Each frame was constructed from a new set of pairs. Initially, frames were refreshed at 50 Hz, later in the series of experiments at 12 Hz. In the rotations, we varied the separation between the elements of a pair (the Glass shift) initially over 1°, 2°, 4°, 8°, 16° and 32° of rotation; later we added 12° and 24°. To correct for the unequal number of presentations, the probabilities in Fig. 1 were calculated as a fraction of the number of times that a shift was used. To stimulate MT cells adequately, we used larger dots than in the psychophysics; the range of shifts was selected such that human observers judged only the centre of the range to be moving. In the translations, the shift was 1°, a value that led to a consistent motion percept in human observers.

In the 'noise' condition, 100 random dots were randomly repositioned at 50 Hz or 12 Hz. In the clockwise and anticlockwise conditions, 100 random dots rotated coherently. The rotation speeds (angular velocity 240° s^{-1}) matched the perceived speed in the Glass patterns. In any experiment, the dot density, extent and luminance were the same for all patterns.

To determine direction tuning, 100 random dots moved on a circular fronto-parallel pathway. This generated motion in all directions and a tuning curve could quickly be generated[11]. Latency was defined as the first 40-ms bin in which an onset response significantly ($P < 0.05$) exceeded the rate in the 200 ms before stimulus onset. To determine the preferred direction (PD), we corrected for the latency, and determined the circular pathway response in 40-ms bins. The PD was defined as the centroid of this activity. The Rayleigh test[20] gave a measure of its significance.

In the interaction paradigms, we combined the circular pathway with Glass patterns or real translations. We called the angle between the PD of the cell and the orientation of the Glass pattern (or the axis of motion for real translation) the conflict angle. Using the axis of motion allowed us to compare the effect of real motion with that of the directionally ambiguous Glass patterns. The change in PD due to the additional pattern was called the deflection. To determine the population deflection, we binned the deflections with respect to the conflict angle (bin width 20°) and averaged over all cells. Its significance was assessed with a Rayleigh test.

Received 13 February; accepted 10 June 2003; doi:10.1038/nature01852.

1. Mishkin, M., Ungerleider, L. & Macko, K. Object vision and spatial vision: two central pathways. *Trends Neurosci.* **6,** 414–417 (1983).
2. Glass, L. Moiré effect from random dots. *Nature* **223,** 578–580 (1969).
3. Ross, J., Badcock, D. R. & Hayes, A. Coherent global motion in the absence of coherent velocity signals. *Curr. Biol.* **10,** 679–682 (2000).
4. Geisler, W. S. Motion streaks provide a spatial code for motion direction. *Nature* **400,** 65–69 (1999).
5. Geisler, W. S., Albrecht, D. G., Crane, A. M. & Stern, L. Motion direction signals in the primary visual cortex of cat and monkey. *Vis. Neurosci.* **18,** 501–516 (2001).
6. Jancke, D. Orientation formed by a spot's trajectory: A two-dimensional population approach in primary visual cortex. *J. Neurosci.* **20,** RC86 (1–6) (2000).
7. Kourtzi, Z. & Kanwisher, N. Activation in human MT/MST by static images with implied motion. *J. Cogn. Neurosci.* **12,** 48–55 (2000).
8. Wilson, H. R., Wilkinson, F. & Asaad, W. Concentric orientation summation in human form vision. *Vision Res.* **37,** 2325–2330 (1997).
9. Burr, D. C. & Ross, J. Direct evidence that 'Speedlines' influence motion mechanisms. *J. Neurosci.* **22,** 8661–8664 (2002).
10. Smith, M. A., Bair, W. & Movshon, J. A. Signals in macaque striate cortical neurons that support the perception of Glass patterns. *J. Neurosci.* **22,** 8334–8345 (2002).
11. Schoppmann, A. & Hoffmann, K.-P. Continuous mapping of direction selectivity in the cat's visual cortex. *Neurosci. Lett.* **2,** 177–181 (1976).
12. Bremmer, F., Ilg, U. J., Thiele, A., Distler, C. & Hoffmann, K. P. Eye position effects in monkey cortex. I. Visual and pursuit-related activity in extrastriate areas MT and MST. *J. Neurophysiol.* **77,** 944–961 (1997).
13. Snowden, R. J., Treue, S., Erickson, R. G. & Andersen, R. A. The response of area MT and V1 neurons to transparent motion. *J. Neurosci.* **11,** 2768–2785 (1991).
14. Qian, N. & Andersen, R. A. Transparent motion perception as detection of unbalanced motion signals. II. Physiology. *J. Neurosci.* **14,** 7367–7380 (1994).
15. Maunsell, J. H. & Van Essen, D. C. Functional properties of neurons in middle temporal visual area of the macaque monkey. I. Selectivity for stimulus direction, speed, and orientation. *J. Neurophysiol.* **49,** 1127–1147 (1983).
16. Albright, T. D. Direction and orientation selectivity of neurons in visual area MT of the macaque. *J. Neurophysiol.* **52,** 1106–1130 (1984).
17. Pack, C. & Born, R. T. Temporal dynamics of a neural solution to the aperture problem in visual area MT of macaque brain. *Nature* **409,** 1040–1042 (2001).
18. Newsome, W. T. & Pare, E. B. A selective impairment of motion perception following lesions of the middle temporal visual area (MT). *J. Neurosci.* **8,** 2201–2211 (1988).
19. Rudolph, K. & Pasternak, T. Transient and permanent deficits in motion perception after lesions of cortical areas MT and MST in the macaque monkey. *Cereb. Cortex* **9,** 90–100 (1999).
20. Batschelet, E. *Circular Statistics in Biology* (Academic, London, 1981).

Supplementary Information accompanies the paper on **www.nature.com/nature**.

Acknowledgements We thank J. Constanza, D. Diep, L. Abavare and M. Bronzel for technical assistance, C. Distler for the surgeries, and G. Stoner and T. Albright for comments and discussions. The Human Frontiers Science Program and the Australian Research Council supported this work financially.

Competing interests statement The authors declare that they have no competing financial interests.

Correspondence and requests for materials should be addressed to B.K. (bart@salk.edu).

Induction of dendritic spines by an extracellular domain of AMPA receptor subunit GluR2

Maria Passafaro[1,2], Terunaga Nakagawa[3], Carlo Sala[2] & Morgan Sheng[3]

[1]*DTI Dulbecco Telethon Institute,*
[2]*CNR Institute of Neuroscience, Cellular and Molecular Pharmacology, Department of Pharmacology, University of Milan, 20129 Italy*
[3]*Picower Center for Learning and Memory, RIKEN-MIT Neuroscience Research Center, Howard Hughes Medical Institute, Massachusetts Institute of Technology, Cambridge, Massachusetts 02139, USA*

Synaptic transmission from excitatory nerve cells in the mammalian brain is largely mediated by AMPA (α-amino-3-hydroxy-5-methyl-4-isoxazole propionic acid)-type glutamate receptors located at the surface of dendritic spines. The abundance of postsynaptic AMPA receptors correlates with the size of the synapse and the dimensions of the dendritic spine head[1–4]. Moreover, long-term potentiation is associated with the formation of dendritic spines as well as synaptic delivery of AMPA receptors[5–8]. The molecular mechanisms that coordinate AMPA receptor delivery and spine morphogenesis are unknown. Here we show that overexpression of the glutamate receptor 2 (GluR2) subunit of AMPA receptors increases spine size and density in hippocampal neurons, and more remarkably, induces spine formation in GABA-releasing interneurons that normally lack spines. The extracellular N-terminal domain (NTD) of GluR2 is responsible for this effect, and heterologous fusion proteins of the NTD of GluR2 inhibit spine morphogenesis. We propose that the NTD of GluR2 functions at the cell surface as part of a receptor–ligand interaction that is important for spine growth and/or stability.

In mature cultured hippocampal neurons (22 days *in vitro*; DIV22), which normally exhibit mushroom-like spines, overexpression of GluR2 increased the length of spines, the width of spine heads and the density of spines (Figs 1 and 2d; see also Supplementary Table 1). In younger neurons (DIV11), GluR2 overexpression induced a higher density of filopodia-like protrusions that were longer and wider than those found on control neurons (Fig. 1; see also Supplementary Table 1). GluR1 overexpression had little effect on the size or number of dendritic spines in DIV22 neurons, and did not induce filopodia-like protrusions in DIV11 neurons (Figs 1 and 2d; see also Supplementary Table 1). Neurons transfected with GluR3 showed spines similar to control green fluorescent protein (GFP)-transfected neurons (Supplementary Table 1). Thus the ability to increase spine number and size seems to be specific for GluR2.

The enlarged spines of GluR2-transfected neurons probably represent bona fide postsynaptic compartments, as they were enriched for F-actin, contained clusters of the postsynaptic density (PSD) proteins Shank and PSD-95, and co-localized with the presynaptic protein bassoon. Indeed, spines of GluR2-overexpressing cells showed increased staining intensity for Shank, PSD-95, F-actin and bassoon, consistent with expansion of the PSD and presynaptic growth (Supplementary Fig. 1).

Which domain(s) of GluR2 are required for its spine-promoting effect? GluR2 mutants lacking the last four amino acids (GluR2Δ4) or the entire cytoplasmic tail (GluR2Δ50) also caused increased spine density and spine-head enlargement (Supplementary Fig. 2 and Table 1), even though the GluR2Δ50 mutant showed reduced surface expression (Supplementary Fig. 3). Thus the carboxy-terminal tail of GluR2, which mediates multiple interactions with